Journal of Radiation Research, Vol. 59, No. 6, 2018, pp. 692–699
doi: 10.1093/jrr/rry075
Advance Access Publication: 20 September 2018

Influence of risk-organ–based tube current modulation on CT-induced DNA double-strand breaks in a biological phantom model

Michael Brand*, Wolfgang Wuest, Matthias May, Michael Uder and Matthias Sommer

Department of Radiology, University Hospital Erlangen, Maximiliansplatz 1, D-91054 Erlangen, Germany
*Corresponding author. Department of Radiology, University Hospital Erlangen, Maximiliansplatz 1, D-91054 Erlangen, Germany. Tel: +49-9131-853-6066; Fax: +49-9131-853-6068; Email: michael.brand@uk-erlangen.de
(Received 7 April 2018; revised 1 July 2018; editorial decision 8 August 2018)

ABSTRACT

Techniques for dose reduction in computed tomography (CT) are receiving increasing attention. Lowering the tube current in front of the patient, known as risk-organ–based tube current modulation (RTM), represents a new approach. Physical dose parameters can determine the exposure but are not able to assess the biological–X-ray interactions. The purpose of this study was to establish a biological phantom model to evaluate the effect of RTM on X-ray–induced DNA double-strand breaks (DSBs). In breast phantoms and in the location of the spine in an Alderson phantom, isolated human blood lymphocytes were irradiated using a 128-slice CT scanner. A standard thoracic CT protocol (120 kV, 110 ref. mAs, anatomy-based tube current modulation, pitch 0.6, scan length 30 cm) with and without RTM was used. X-ray–induced DSBs were quantified in isolated blood lymphocytes using immunofluorescence microscopy after staining for the phosphorylated histone variant γ-H2AX. Using RTM, the resulting DNA damage reduction was 41% in superficial breast locations ($P = 0.0001$), 28% in middle breast locations ($P = 0.0003$) and 29% in lower breast locations ($P = 0.0001$), but we found a DNA damage increase of 36% in superficial spine locations ($P = 0.0001$) and of 26% in deep spine locations ($P = 0.0001$). In summary, we established a biological phantom model that is suitable for detecting DNA damage in distinct organs. In addition, we were able to show that, using RTM, X-ray–induced DNA damage in the breast can be significantly reduced; however, there is a significant increase in DSBs in the location of the spine.

Keywords: DNA double-strand breaks (DSBs); γ-H2AX; risk-organ–based tube current modulation (RTM); computed tomography (CT)

INTRODUCTION

Computed tomography (CT) contributes the major proportion to radiation exposure in diagnostic imaging [1–3]. Therefore, techniques for dose reduction are receiving increasing attention. Several techniques (like anatomy-based tube current modulation, low-kV protocols, and—particularly used in cardiac CT—ECG-triggered tube current modulation and high-pitch protocols) are already in use [4–6]. Risk-organ–based tube current modulation (RTM) is a rather new approach in CT, and it is supposed to reduce the dose to radiation-sensitive risk organs such as the female breast. RTM is based on lowering the tube current while the X-ray tube is in front of the patient, but increasing it when it is to the rear of the patient to maintain image quality. Estimation of the delivered radiation dose during CT is based on physical measurements using ionization chambers, mathematical analyses (e.g. Monte-Carlo simulation) and calculation of exposure parameters like computed tomography dose index (CTDI) or dose length product (DLP) [1, 7–9]. However, the biological radiation effects not only depend on the radiation dose, but are also reliant on individual patient factors like age and DNA repair capacity, and the application of contrast medium [4, 6, 9–15]. γ-H2AX immunofluorescence microscopy is a sensitive technique for determining X-ray–induced DNA double-strand

breaks (DSB) *in vitro* and *in vivo*. Previous studies demonstrated a very good correlation between radiation dose and the resulting γ-H2AX foci representing distinct DSBs in human blood lymphocytes after CT, angiography or cardiac catheter examination [12, 16–19]. However, in those studies peripheral blood lymphocytes were used to assess radiation damages; that technique, however, is not suitable for evaluation of the effect of RTM because in this case the radiation effects on the organ are more of interest than the effects on the whole body. Therefore, the aim of this study was to establish a biological phantom model for estimation of the X-ray–induced γ-H2AX foci in radiation-sensitive organs, and to evaluate the effect of RTM.

MATERIALS AND METHODS

The study complies with the Declaration of Helsinki and was performed following local ethics committee approval. Written informed consent was obtained from every volunteer.

Preparation of blood samples

For the *in vitro* experiments, blood samples from three healthy volunteers (median age: 33.2 years, range 27–38 years) with no history of cancer, chemotherapy or leukemia and without exposure to ionizing radiation within the last 3 days were used. Thirty milliliters of blood was obtained from the antecubital vein of each individual using ethylenediaminetetraacetic acid (EDTA)-containing vials.

To isolate human blood lymphocytes, blood was layered onto lymphocyte separation medium 1077 (Biochrom, Berlin, Germany) and centrifuged at 1200*g* for 15 min at a temperature of 37°C. Cells from the resulting interphase containing ~80% lymphocytes [17] were resuspended in a solution containing 80% Roswell Park Memorial Institute (RPMI) medium 1640 (Biochrom, Berlin, Germany) and 20% fetal calf serum (FCS). These cells were washed and centrifuged twice at 300*g* and once at 240*g*, respectively for 10 min, resuspended in phosphate buffered saline (PBS) (ph 7.1) and distributed into small (2 µl) plastic tubes. The separation and washing processes lasted ~50–60 min and were performed at 37°C.

Phantom model and CT protocols

For the exposure, a 128-slice CT-Scanner (Siemens Definition Flash, Siemens Healthcare, Forchheim, Germany) was used. To establish the phantom model we used a commercially available 32 cm CTDI-phantom. Tubes containing 1 µl of isolated lymphocyte suspension were placed in the central and in the peripheral boreholes of the phantom. We irradiated the lymphocytes using a standard chest CT protocol (tube voltage 120 kV, pitch 0.6, rotation time 0.28 s) at different tube currents of 50, 100, 150, 200 and 250 mAs without anatomy-based or risk-organ–based tube current modulation. The scan range was 10 cm. This experiment was performed in triplicate.

For evaluation of the risk-organ–based tube current modulation (RTM), an Alderson chest phantom was positioned precisely at a defined height (center of the gantry) by using the localization system of the CT scanner with commercially available breast essays. The breast phantoms consist of three slices of 2.5 cm thickness, each with several boreholes (Fig. 1a and b). Tubes containing 1 µl of lymphocyte suspension were placed in various superficial (Locations 1–4), middle (Locations 5–6) and deep locations (Locations 7–10) in the breast phantoms (Fig. 1a). To evaluate the effect of RTM on the dorsal parts of the body, lymphocyte-containing tubes were placed in three consecutive slices in deep (Locations R1, R3 and R5) and superficial spine locations (Locations R2, R4 and R6) at the same height as the breast locations (Fig. 1b). These experiments were also performed in triplicate. Non-irradiated lymphocytes were used as controls to determine the γ-H2AX baseline levels ($n = 3$). The lymphocytes were exposed to X-rays using a standard chest CT protocol as shown in Table 1, either with or without RTM (X-Care, Siemens Healthcare, Forchheim, Germany). The scan range was 30 cm. Using RTM, the tube current was reduced ~40% at an angle of 130° when the tube was in front of the patient. To maintain the image quality, the tube current was increased while the tube was to the rear of the patient. In every experiment, the standard anatomy-based tube current modulation (Care Dose 4D, Siemens Healhcare, Forchheim, Germany) was used. $CTDI_{vol}$ and DLP were registered as provided by the patient protocol (Table 2).

Immunofluorescent work-up of the exposed blood lymphocytes

At 5 min after irradiation, samples were stored at 4°C during transport to the laboratory and work-up was performed immediately. Lymphocyte samples were layered onto microscope slides for 10 min at room temperature, followed by fixation in 100% methanol (20 min, at −20°C) and permeabilization in 100% acetone (1 min, at −20°C). All microscope slides were washed three times in PBS containing 1% FCS for 10 min. The fixation process lasted ~40 min.

To quantify the DNA DSBs, staining of the early phosphorylated histone variant H2AX was used. After overnight incubation with a specific γ-H2AX antibody (Anti-H2A.X-Phosphorylated (Ser 139), BioLegend, Uithoorn, The Netherlands) at a concentration of 1:2500 at 4°C, and after washing (3 × 10 min) with PBS containing 1% FCS, the microscope slides were stored for fixation in 2.5% formaldehyde for 20 min (−20°C). Each sample was washed three times for 10 min in PBS containing 1% FCS and incubated with Alexa Fluor 488-conjugated goat antimouse secondary antibody (Invitrogen, Paisley, UK) at a dilution of 1:400 for 1 h at room temperature. The lymphocytes were washed 4 × 10 min in PBS (pH 7.1) and mounted with VECTASHIELD® mounting medium containing 4,6-diamidino-2-phenylindole (Vector Laboratories, Burlingame, USA).

γ-H2AX immunofluorescence microscopy

Fluorescence analysis was performed using an Axioplan 2 microscope (Carl Zeiss, Jena, Germany) equipped with a ×63 magnification objective. In each sample, lymphocytes were counted until 40 foci were detected, and the γ-H2AX foci numbers were related to the number of enumerated cells (each γ-H2AX focus represents one DSB). To determine the number of X-ray–induced DNA DSBs (excess foci), pre-exposure foci levels were subtracted from the number of foci obtained after irradiation. The foci of each microscope slide were quantified three times, and each microscope slide

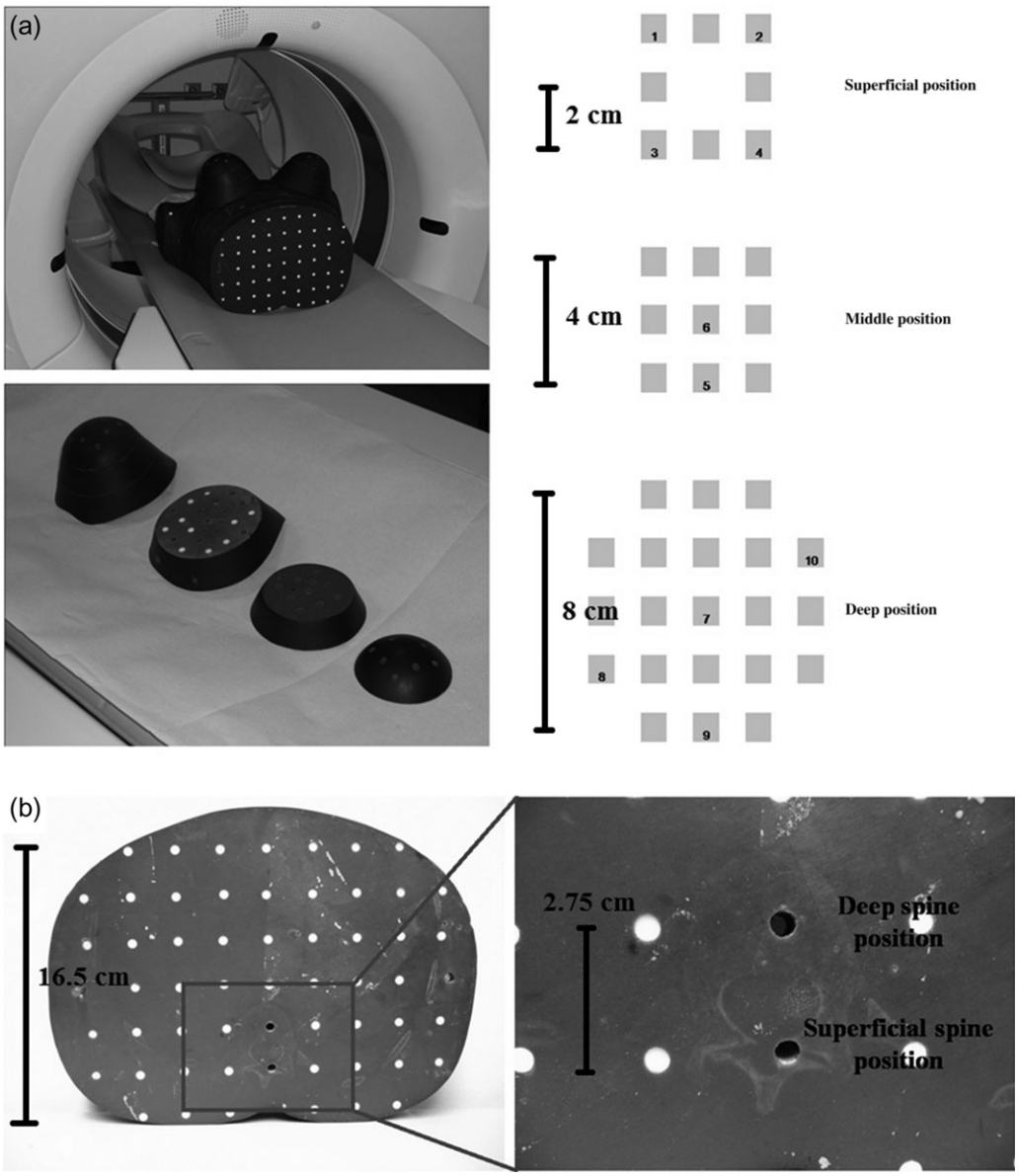

Fig. 1. Set-up for *in vitro* testing: On the left panel of Fig. 1a, the Alderson chest phantom and the three slices of the breast phantoms are shown. The Alderson Phantom was placed in the center of the CT-scanner, and the breast phantoms were positioned on the chest. The right panel demonstrates the locations of the lymphocyte samples in the different boreholes for the distinct slices of the breast essays. For each experiment, we placed four lymphocytes samples in the superficial slice (Numbers 1–4), two in the middle slice (Numbers 5–6) and four in the deep slice (Numbers 7–10) in various locations. In Fig. 1b, the spinal sample locations are shown. Two samples were placed in three consecutive slices corresponding to the breast phantoms (deep locations: R1, R3, R5; superficial locations: R2, R4, R6).

was evaluated independently by two blinded persons with 6 and 11 years of experience in γ-H2AX immunofluorescence microscopy.

Statistical analysis

Statistical analyses were performed using the software Prism 4.03, 2005 (Graph-Pad Software, San Diego, CA). The Spearman correlation was calculated between excess foci levels and the tube current time product. In order to compare DSB levels in different locations in the Alderson phantom with and without RTM, the paired *t*-test was used. A *P*-value <0.05 was considered to be statistically significant.

RESULTS

The pre-exposure mean γ-H2AX foci levels in the blood samples were 0.077 DSBs/cell $\pm$ 0.015 and were used to determine the number of X-ray–induced DNA DSBs (excess foci): the pre-exposure

Table 1. Scan protocols: this table shows the scan parameters of the standard chest CT protocol without and with RTM

	Thoracic CT protocol without RTM	Thoracic CT protocol with RTM
Tube current time product (effective mAs)	110	110
Tube voltage (kV)	120	120
Pitch	0.6	0.6
Rotation time (s)	0.28	0.28
Scan time (s)	4.18	4.18
Anatomy-based tube current modulation	+	+
Scan length (mm)	300	300
Risk-organ–based tube current modulation	−	+

Table 2. Exposure protocols: this table shows the exposure parameters for thoracic CT protocols with and without RTM, as used for the Alderson phantom experiments

	Thoracic CT protocol without RTM	Thoracic CT protocol with RTM
Reference mAs	110	110
Resulting mAs	95	110
CTDIvol (mGy)	6.44	7.51
DLP (mGy × cm)	214	227

foci levels were subtracted from the number of foci obtained after irradiation.

A significant increase in γ-H2AX foci was obtained after X-ray exposure—regardless of central or peripheral location in the CTDI-Phantom, but the increase in foci was higher in peripheral compared with central samples. The mean excess foci ranged from 0.037 DSBs/cell (50 mAs) to 0.176 DSBs/cell (250 mAs) in the central, and from 0.046 DSBs/cell (50 mAs) to 0.220 DSBs/cell (250 mAs) in the peripheral samples. Both for central ($r = 0.9906$; $P = 0.0011$) and peripheral locations ($r = 0.9911$, $P = 0.0010$), a significant correlation was obtained between the excess foci and the tube current time product (Fig. 2).

There was only a non-significant, slight increase in the DLP using RTM (Table 2). Regardless of the locations in the breast of the Alderson Phantom we detected significantly fewer excess foci when using RTM in all samples compared with in samples exposed without RTM (see Figs 3a and 4a); thereby, we also observed a dependence of excess foci from the sample location in the breast phantoms. The means of the excess foci were 0.165 DSBs/cell ± 0.026 without RTM and 0.098 DSBs/cell ± 0.013 with RTM ($P = 0.0001$) in superficial locations (1–4), 0.106 DSBs/cell ± 0.014/cell without RTM and 0.076 DSBs/cell ± 0.008 with RTM ($P = 0.0003$) in middle locations (5–6), and 0.059 DSBs/cell ± 0.009 without RTM and 0.042 DSBs/cell ± 0.008 with RTM ($P = 0.0001$) in deep locations (7–10) (Fig. 3a and left panel of Fig. 4a). The resulting DNA damage reduction was 41% in superficial locations, 28% in middle locations and 29% in lower locations (see left panel of Fig. 4b). Furthermore, mean excess foci were 0.126 DSBs/cell ± 0.014 without RTM and 0.172 DSBs/cell ± 0.014 with RTM ($P = 0.0001$) in superficial spine locations (R2, R4 and R6) and 0.078 DSBs/cell ± 0.014 without RTM and 0.098 DSBs/cell ± 0.013 with RTM ($P = 0.0001$) in deep spine locations (R1, R3 and R5) (see Fig. 3b + 4a right panel). Using RTM, we obtained a DNA damage increase of 36% in superficial spine locations (R2, R4 and R6) and of 26 % in deep spine locations (R1, R3 and R5) (Fig. 4b right panel).

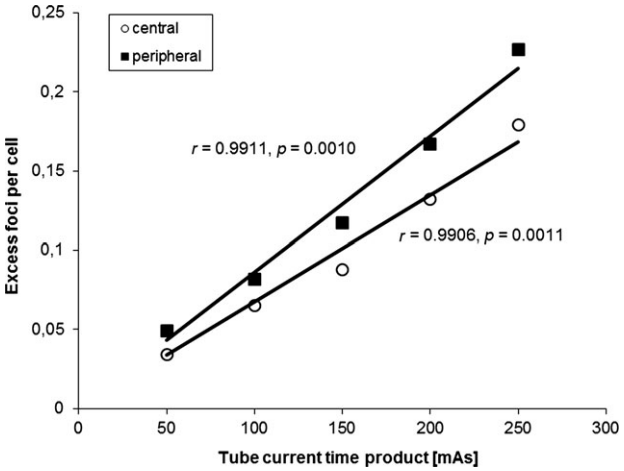

Fig. 2. Set-up for establishment of the phantom model using the CTDI phantom: a standard chest CT protocol with a constant tube voltage of 120 kV and various tube current time products without anatomy-based or risk-organ–based tube current modulation. The *x*-axis shows the tube current time product, the *y*-axis represent the excess foci levels. The Pearson correlation (*r*), both for the peripheral (squares) and the central locations (circles) are shown. The figure illustrates the mean excess foci of three independent measurements. A *P*-value <0.05 was considered statistically significant.

DISCUSSION

We established a biological *in vitro* phantom model for estimation of CT-induced DSBs in distinct organs. Independently of the use of RTM, we detected the highest foci levels in superficial locations, followed by middle and deep locations, which can be explained by absorption of X-rays in the breast tissue. With RTM, a DSB reduction could be obtained in superficial locations (~41%), followed by middle and deep locations (~30%). Compared with a standard thoracic CT, an increase in DSBs was found in superficial (36.5%) and deep spine locations (26%), due to an increase in the tube current

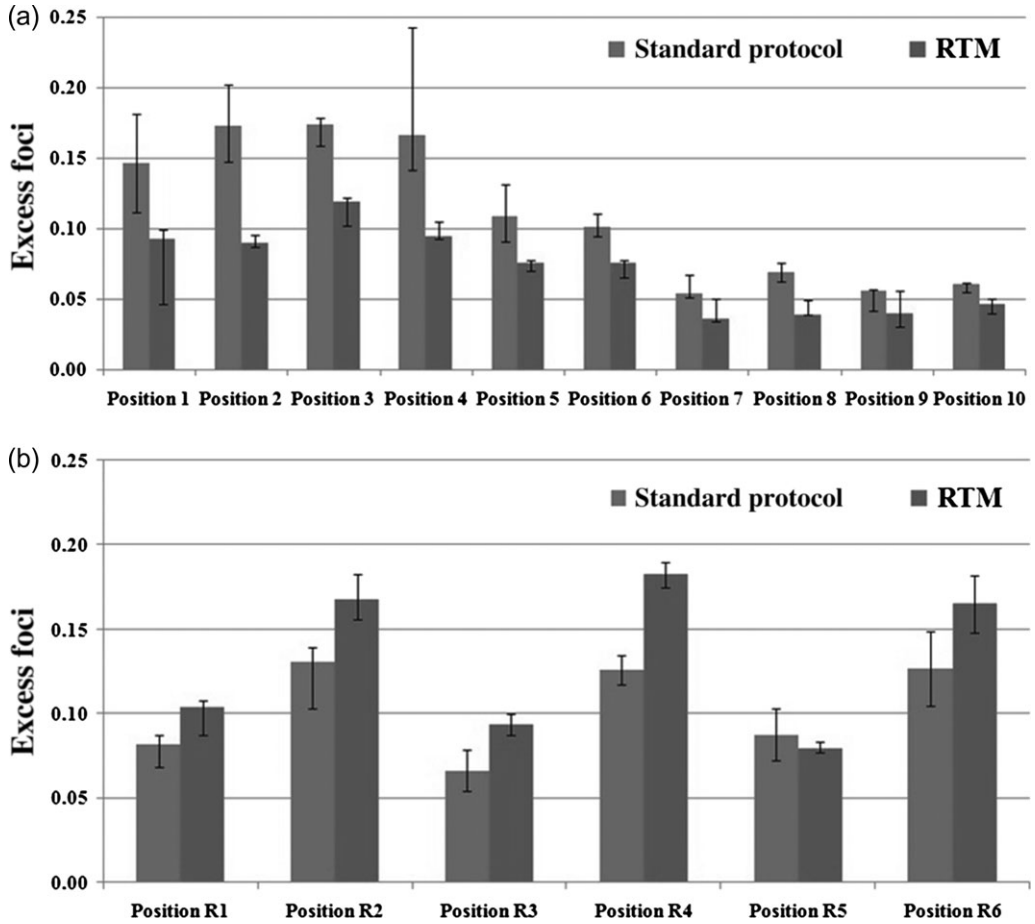

Fig. 3. Excess foci in all of the distinct tested sample locations in the Alderson phantom: (a) shows the values of the breast phantoms, locations correspond to the locations of Fig. 1a; (b) demonstrates values in the spine locations in three consecutive slices of the chest phantom (R1, R3 and R5: deep position; R2, R4 and R6: superficial position). The black columns show samples irradiated using the standard protocol without RTM; the grey columns indicate samples irradiated using RTM. Columns represent mean excess foci; error bars indicate standard deviation.

to the rear of the patient. This increase can be explained by the fact that there is an increase in the tube current when the tube is behind the patient. This is necessary in order to maintain image quality. Overall, higher DSB levels were obtained in superficial than in deep locations, which can be explained by X-ray absorption.

In various previous studies, a similar decrease in the radiation dose by RTM was reported but, in contrast, we are the first group that has used a biological model. Vollmar *et al.* studied the effect of organ-based–risk tube current modulation using the Monte Carlo simulation and reported a dose reduction of 47.8% in the chest and an increase in the bone marrow of 17.9% [9]. Duan *et al.* observed similar effects with an anthropomorphic phantom. Using an ionization chamber, they determined a dose reduction of 38.1% for the anterior region and an increase of 24.7 % for the posterior parts of the body [20]. Finally Wang *et al.* found a dose reduction of 34–39% for the risk organ–based tube current modulation using a semianthropomorphic phantom [21]. Our results are in line with those studies, but there has been a recent study by Franck *et al.* that showed there is only a 9% dose reduction in the female breast, in contrast to our results [22]. This difference can be explained in that, in their study, not all breast tissue was within the reduced tube current zone, and therefore the effect was not as big as if the breast tissue was within the reduced tube current zone. Interestingly, the increase in the radiation dose in the spine location was similar to our increase in DSBs in the spine location (26% vs 26–36.5%); this can be explained because, compared with the female breast, the spine has less anatomical variants in size and shape. Fu *et al.* showed that depending on the female breast location, there are differing amounts of radiation exposure: if the breast tissue is within the reduced tube current zone, then a dose reduction of ~40% was detected, which is in line with our results [23].

The immunofluorescence microscopy method, based on the phosphorylation of the histone variant H2AX, can be used for quantification of DNA DSBs during various radiologic techniques, including CT and angiography, and it is well established [4, 6, 11–14, 17–19]. A significant correlation between the numbers of

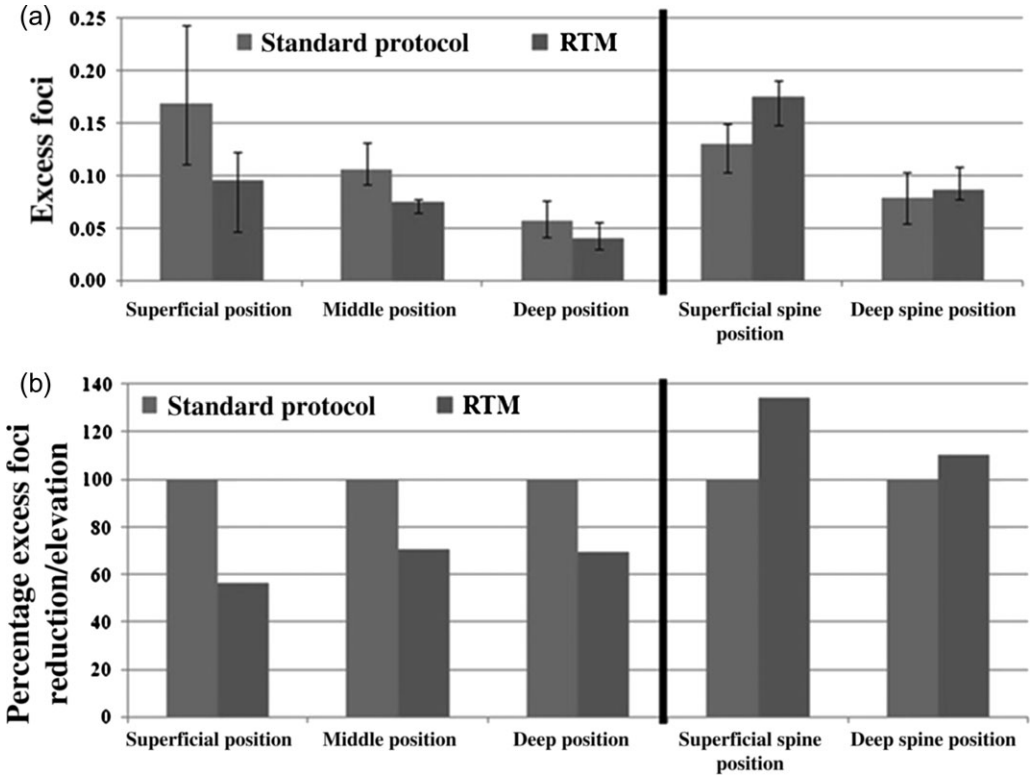

Fig. 4. Dependency of excess foci on the sample locations in the phantom: Part (a) shows mean excess foci of samples placed in the superficial, middle and deep slices of the breast phantoms, and in the superficial and deep spine locations in the chest phantom. Means (columns) and standard deviation (error bars) of each slice are presented. Part (b) shows the percentage of DSB reduction/elevation in RTM in comparison with the standard thoracic protocol. For this illustration, the values of the samples irradiated without RTM, as shown in panel (a), were considered to be 100%. The black columns show samples irradiated using the standard protocol without RTM; the grey columns indicate samples irradiated using RTM.

X-ray–induced γ-H2AX foci and the dose deposited *in vitro* and *in vivo* has been found [4, 5, 13, 24, 25]. Each H2AX focus represents one DSB. DSBs are considered to be the most significant DNA lesions induced by ionizing radiation. Previously, it has been shown in a mouse model that induction of DSBs is comparable between different cell types [19, 26]. After X-ray exposure, induced DSBs can be observed within 5 min [4, 5, 17, 19, 24]. This method is able to detect DNA damage after low radiation exposure (<1 mGy). Therefore, it provides a reliable and sensitive technique for quantification of acute DNA damage [4, 6, 10–12, 17, 18]. However, in all of these studies γ-H2AX foci were evaluated in peripheral blood lymphocytes. This approach would not be appropriate for the evaluation of the effect of RTM because this dose-reducing technique, rather than having a systemic effect, has a local effect on the exposed organs. Therefore, we decided to adapt the γ-H2AX immunoflourescence method to estimate the local DNA damage in distinct organs using an Alderson phantom. For the establishment of our phantom model, we performed experiments using a CTDI phantom and obtained a significant correlation between the excess foci levels and the DLP in the tested dose range ($r = 0.9906$; $P = 0.0011$), confirming the reliability of our approach.

There are also some limitations to this study that have to be mentioned. We only performed *in vitro* experiments, simulating the *in vivo* situation, because due to ethical reasons and the risk for the patients it is not possible to obtain tissue samples from individuals undergoing thoracic CT. The setting of the study is experimental and the data represent only estimations of the real DNA damage in breast tissue, and we used a standard Alderson phantom, so we cannot describe the effect of the constitution (thin vs obese bodies). In addition, the breast essays of the Alderson phantom do not represent the individual differences in size or amount of glandular tissue. The complete breast tissue is not located within the angle of 130° in all women, the angle within which the tube current is lowered; thus, all breast tissue is not protected by the tube current reduction in every case (e.g. this may not be the case in obese patients); whether a bra can improve this situation should be investigated in further studies.

It is important to note that damage in peripheral blood lymphocytes is not the same as cancer induction. Therefore, γ-H2AX foci after *ex vivo* irradiation of lymphocytes in peripheral blood may not be taken as a surrogate for cancer induction by radiation exposure, even if increased DSB turnover might statistically be associated with

an increased rate of DNA misrepair. γ-H2AX immunofluorescence microscopy is a time-consuming and expensive method. No reliable automated scoring system is available so far that avoids a routine analysis in a bigger study population. Finally, we only assessed the effect of RTM on the biological radiation effects, and did not evaluate the image quality because this was beyond the scope of our study. However, in a recent paper, the overall image quality was not significantly different between chest CTs with and without RTM [27].

CONCLUSION

In conclusion, the established biological phantom model is suitable for estimation of X-ray–induced γ-H2AX foci representing DNA DSBs in organs. Using this approach, we were able to show a significant DSB reduction in breast locations but also a significant increase in DSBs in spine locations using RTM. With the established phantom model, the effect of other dose reduction tools (e.g. bismuth shields) or scan modes can be studied in future.

CONFLICT OF INTEREST

There are no potential conflicts of interest to disclose.

FUNDING

No funding has been received for the work.

REFERENCES

1. Angel E, Yaghmai N, Jude CM et al. Dose to radiosensitive organs during routine chest CT: effects of tube current modulation. *Am J Roentgenol* 2009;193:1340–5. doi:10.2214/AJR.09.2886.
2. Haaga JR. Radiation dose management: weighing risk versus benefit. *AJR Am J Roentgenol* 2001;177:289–91.
3. Mettler FA Jr., Wiest PW, Locken JA et al. CT scanning: patterns of use and dose. *J Radiol Prot* 2000;20:353–9.
4. Kuefner MA, Grudzenski S, Hamann J et al. Effect of CT scan protocols on x-ray–induced DNA double-strand breaks in blood lymphocytes of patients undergoing coronary CT angiography. *Eur Radiol* 2010;20:2917–24. doi:10.1007/s00330-010-1873-9.
5. Brand M, Sommer M, Achenbach S et al. X-ray induced DNA double-strand breaks in coronary CT angiography: comparison of sequential, low-pitch helical and high-pitch helical data acquisition. *Eur J Radiol* 2012;81:e357–62. doi:10.1016/j.ejrad.2011.11.027.
6. Kuefner MA, Hinkmann FM, Alibek S et al. Reduction of X-ray induced DNA double-strand breaks in blood lymphocytes during coronary CT angiography using high-pitch spiral data acquisition with prospective ECG-triggering. *Invest Radiol* 2010;45:182–7. doi:10.1097/RLI.0b013e3181d3eddf.
7. Deak P, van Straten M, Shrimpton PC et al. Validation of a Monte Carlo tool for patient-specific dose simulations in multislice computed tomography. *Eur Radiol* 2008;18:759–72. doi:10.1007/s00330-007-0815-7.
8. Kalender WA, Schmidt B, Zankl M et al. A PC program for estimating organ dose and effective dose values in computed tomography. *Eur Radiol* 1999;9:555–62.
9. Vollmar SV, Kalender WA. Reduction of dose to the female breast in thoracic CT: a comparison of standard-protocol, bismuth-shielded, partial and tube-current-modulated CT examinations. *Eur Radiol* 2008;18:1674–82. doi:10.1007/s00330-008-0934-9.
10. Beels L, Bacher K, De Wolf D et al. γ-H2AX foci as a biomarker for patient X-ray exposure in pediatric cardiac catheterization: are we underestimating radiation risks? *Circulation* 2009;120:1903–9. doi:10.1161/CIRCULATIONAHA.109.880385.
11. Kuefner MA, Grudzenski S, Schwab SA et al. DNA double-strand breaks and their repair in blood lymphocytes of patients undergoing angiographic procedures. *Invest Radiol* 2009;44:440–6. doi:10.1097/RLI.0b013e3181a654a5.
12. Nazarov IB, Smirnova AN, Krutilina RI et al. Dephosphorylation of histone gamma-H2AX during repair of DNA double-strand breaks in mammalian cells and its inhibition by calyculin A. *Radiat Res* 2003;160:309–17. doi:RR3043 [pii].
13. Rothkamm K, Balroop S, Shekhdar J et al. Leukocyte DNA damage after multi-detector row CT: a quantitative biomarker of low-level radiation exposure. *Radiology* 2007;242:244–51. doi:10.1148/radiol.2421060171.
14. Grudzenski S, Kuefner MA, Heckmann MB et al. Contrast medium-enhanced radiation damage caused by CT examinations. *Radiology* 2009;253:706–14. doi:10.1148/radiol.2533090468.
15. Piechowiak EI, Peter JF, Kleb B et al. Intravenous iodinated contrast agents amplify DNA radiation damage at CT. *Radiology* 2015;275:692–7. doi:10.1148/radiol.14132478.
16. Antonelli F, Belli M, Cuttone G et al. Induction and repair of DNA double-strand breaks in human cells: dephosphorylation of histone H2AX and its inhibition by calyculin A. *Radiat Res* 2005;164:514–7. doi:RR3379 [pii].
17. Lobrich M, Rief N, Kuhne M et al. *In vivo* formation and repair of DNA double-strand breaks after computed tomography examinations. *Proc Natl Acad Sci U S A* 2005;102:8984–9. doi:10.1073/pnas.0501895102.
18. Rogakou EP, Pilch DR, Orr AH et al. DNA double-stranded breaks induce histone H2AX phosphorylation on serine 139. *J Biol Chem* 1998;273:5858–68.
19. Rothkamm K, Lobrich M. Evidence for a lack of DNA double-strand break repair in human cells exposed to very low x-ray doses. *Proc Natl Acad Sci U S A* 2003;100:5057–62. doi:10.1073/pnas.0830918100.
20. Duan X, Wang J, Christner JA et al. Dose reduction to anterior surfaces with organ-based tube-current modulation: evaluation of performance in a phantom study. *Am J Roentgenol* 2011;197:689–95. doi:10.2214/AJR.10.6061.
21. Wang J, Duan X, Christner JA et al. Radiation dose reduction to the breast in thoracic CT: comparison of bismuth shielding, organ-based tube current modulation, and use of a globally decreased tube current. *Med Phys* 2011;38:6084–92. doi:10.1118/1.3651489.
22. Franck C, Smeets P, Lapeire L et al. Estimating the patient-specific dose to the thyroid and breasts and overall risk in chest

CT when using organ-based tube current modulation. *Radiology* 2018;288:164–9. doi:10.1148/radiol.2018170757.

23. Fu W, Tian X, Sturgeon GM et al. CT breast dose reduction with the use of breast positioning and organ-based tube current modulation. *Med Phys* 2017;44:665–78. doi:10.1002/mp.12076.
24. Kuefner MA, Brand M, Ehrlich J et al. Effect of antioxidants on X-ray–induced gamma-H2AX foci in human blood lymphocytes: preliminary observations. *Radiology* 2012;264:59–67. doi:10.1148/radiol.12111730.
25. Rube CE, Grudzenski S, Kuhne M et al. DNA double-strand break repair of blood lymphocytes and normal tissues analysed in a preclinical mouse model: implications for radiosensitivity testing. *Clin Cancer Res* 2008;14:6546–55.doi:10.1158/1078-0432.CCR-07-5147.
26. Rube CE, Dong X, Kuhne M et al. DNA double-strand break rejoining in complex normal tissues. *Int J Radiat Oncol Biol Phys* 2008;72:1180–7. doi:10.1016/j.ijrobp.2008.07.017.
27. Kim YK, Sung YM, Choi JH et al. Reduced radiation exposure of the female breast during low-dose chest CT using organ-based tube current modulation and a bismuth shield: comparison of image quality and radiation dose. *Am J Roentgenol* 2013; 200:537–44. doi:10.2214/AJR.12.9237.